

Protective Effects of SIRT2 Inhibition on Cardiac Fibrosis

ABSTRACT

Background: A primary factor in the pathogenesis of aging is oxidative stress, with cardiac inflammation and fibrosis being contributed to by increased oxidative stress as organisms age. Oxidative stress enhances the cardiac fibrotic signaling pathway, with reactive oxygen species inducing cardiac fibrosis through increased expression of the profibrotic factor transforming growth factor-beta 1 (TGF- β 1). Furthermore, Wnt/ β -catenin signaling pathway is implicated in interstitial fibrosis, which is associated with TGF- β . Sirtuin 2 (SIRT2) is expressed in heart tissue, with protective effects in pathological cardiac hypertrophy. We aimed to investigate the mechanisms of cardiac fibrosis in D-Galactose (D-Gal)-induced accelerated aging, focusing on TGF- β 1, β -catenin, and SIRT2.

Methods: A total of 30 young male Sprague–Dawley rats were randomly divided into 4 groups: control group, D-Gal group, D-Gal + 4% dimethyl sulfoxide (DMSO) group, and D-Gal + the SIRT2 inhibitor (AGK2) group. After 10 weeks, the rats were sacrificed, and their hearts were removed. SIRT2 expression levels were measured by western blot and gene expression levels of TGF- β 1 and β -catenin by quantitative real-time polymerase chain reaction.

Results: Transforming growth factor-beta 1 (TGF- β 1) mRNA expression in heart tissue was higher in the D-Gal group compared to all other groups. β -catenin mRNA expression was higher in the D-Gal group than in the D-Gal + AGK2 group. SIRT2 protein expression was higher in the D-Gal + DMSO group compared to the control group. Sirtuin 2 expression was lower in the D-Gal + AGK2 group compared to the D-Gal and D-Gal + DMSO groups.

Conclusion: Sirtuin 2 inhibition attenuates fibrosis, as evidenced by the downregulation of TGF- β 1 and β -catenin. Thus, targeting SIRT2 may represent a potential therapeutic strategy for diseases characterized by cardiac fibrosis in the future.

Keywords: Animal model, β -catenin, cardiac fibrosis, SIRT2, TGF- β 1

INTRODUCTION

Cardiovascular diseases (CVD) constitute the leading cause of mortality among the elderly.¹ Advancing age is a risk factor for the development and progression of CVD. Cardiac hypertrophy is one of the most prevalent cardiovascular alterations resulting from aging. Aging is a risk factor for cardiac hypertrophy and fibrosis that can eventually lead to heart failure.²

Chronic administration of D-galactose (D-Gal) induces accelerated aging in rodents, closely mimicking natural aging processes.^{3,4} Research indicates that 3-month-old rats treated with D-Gal demonstrate structural and functional traits comparable to those of 16 24-month-old rats, effectively mimicking natural aging. Furthermore, studies demonstrate that D-Gal administration impairs the diastolic functions of the heart, thereby functioning as a model for age-related cardiomyopathy.^{5,6}

In the heart and brain, elevated levels of D-Gal can be converted into aldose and hydrogen peroxide via galactose oxidase catalysis, resulting in the production of reactive oxygen species (ROS). This process leads to oxidative stress, inflammation, mitochondrial dysfunction, and apoptosis.⁷ Administration of D-Gal to mice and rats aged 2–5 months at doses of 60–150 mg/kg/day for 6–8 weeks increased aging markers such as protein DNA oxidation and lipid peroxidation in heart

ORIGINAL INVESTIGATION

Müge Akbulut¹ 

Arzu Keskin Aktan² 

Gizem Sonugür³ 

Saadet Özen Akarca⁴ 

Aslı Nur Bahar⁵ 

Hatice Kavak⁴ 

Gonca Akbulut⁴ 

¹Department of Cardiology, Ankara University Faculty of Medicine, Ankara, Türkiye

²Department of Physiology, Afyon Kocatepe University Faculty of Medicine, Afyon, Türkiye

³Department of Basic Oncology, Ankara University Cancer Research Institute, Ankara, Türkiye

⁴Department of Physiology, Gazi University Faculty of Medicine, Ankara, Türkiye

⁵Department of Physiology, Marmara University Faculty of Medicine, İstanbul, Türkiye

Corresponding author:

Müge Akbulut
✉ iremuge@yahoo.com

Received: September 4, 2024

Accepted: December 11, 2024

Available Online Date: January 29, 2025

Cite this article as: Akbulut M, Keskin Aktan A, Sonugür G, et al. Protective effects of sirtuin 2 inhibition on cardiac fibrosis. *Anatol J Cardiol.* 2025;29(4):173–180.



Copyright©Author(s) - Available online at anatoljcardiol.com.
Content of this journal is licensed under a Creative Commons Attribution-NonCommercial 4.0 International License.

DOI:10.14744/AnatolJCardiol.2025.4770

tissue.³ Oxidative stress is a primary factor in the pathogenesis of aging, with increased oxidative stress contributing to cardiac inflammation and fibrosis as organisms age.⁸ Cardiac fibrosis is characterized by the inappropriate deposition of extracellular matrix components, including collagen and fibronectin.⁹

At the molecular level, transforming growth factor-beta (TGF- β) is a key regulator of profibrotic processes. Its elevated levels in cardiac fibrosis in both humans and animals highlight its importance.^{10,11} Transforming growth factor-beta triggers the phenotypic transition of cardiac fibroblasts to myofibroblasts, and the disruption or inhibition of TGF- β signaling has been shown to have protective effects in animal models.¹⁰

The increase in ROS is associated with heightened levels of matrix metalloproteinases and TGF- β , as well as abnormal glucose oxidation, all of which contribute to the progression of cardiac fibrosis.¹² Oxidative stress enhances the cardiac fibrotic signaling pathway, with ROS inducing cardiac fibrosis through increased expression of the profibrotic factor transforming growth factor-beta 1 (TGF- β 1) expression.^{9,12} Transforming growth factor-beta is pivotal in the activation of resident cardiac fibroblasts and promotes extracellular matrix production via Smad2/3 signaling pathways in response to diverse stimuli.¹³

The Wnt/ β -catenin signaling pathway is closely related to cellular senescence, and continuous Wnt exposure has been shown to accelerate cellular aging both in vivo and in vitro.¹⁴ There is a mechanistic link between Wnt signaling and the heart diseases observed in the elderly, with Wnt activation promoting the transformation of fibroblasts into active fibroblasts or myoblasts, thereby contributing to cardiac fibrosis in the aged heart.¹⁵ The canonical Wnt/ β -catenin signaling pathway is implicated in myocardial hypertrophy¹⁶ and interstitial fibrosis,¹⁷ both of which are associated with TGF- β . Recent research has shown that TGF- β induces the production and secretion of canonical Wnt proteins and activates β -catenin in cardiac fibroblasts.¹⁸

Sirtuins (SIRT1-7) constitute a family of class III histone deacetylases involved in metabolic control, apoptosis, cell survival, inflammation, and healthy aging. Sirtuin 2 is expressed in a variety of metabolically active tissues, including the heart, brain, and adipose tissue. D-Galactose administration has been shown to increase SIRT2 levels in the brain,¹⁹ liver,²⁰ and kidney.²¹ Recent studies have shown that

SIRT2 is involved in cardiac hypertrophy²² and heart failure,²³ but this role is unclear. While the protective effects of SIRT2 in pathological cardiac hypertrophy have been shown,^{22,24} it has also been shown that downregulation of SIRT2 is protective in ischemia-reperfusion.²⁵ Likewise, the activation of SIRT3 has been shown to be associated with the inhibition of TGF- β synthesis.²⁶

Additionally, numerous frequently prescribed cardiovascular drugs demonstrate pleiotropic effects through epigenetic mechanisms, such as histone modification and alterations in the expression of various genes. For instance, statins modulate SIRT1 transcription and elicit epigenetic modifications, leading to anti-inflammatory and apoptotic pathways. Similarly, metformin, sodium-glucose cotransporter-2 inhibitors, and hydralazine also exhibit similar epigenetic mechanisms.²⁷

Treatment options for cardiac hypertrophy are limited, and few therapies directly target cardiac function and remodeling.²⁸ There is a need for a deeper understanding of the molecular mechanisms underlying cardiac hypertrophy in order to develop new therapeutic strategies that can slow the progression of heart disease or prevent it. This study aims to investigate the mechanisms of cardiac fibrosis in D-Gal-induced accelerated aging, focusing on TGF- β 1, β -catenin, and SIRT2.

METHODS

Animals

All rats were housed under standard laboratory conditions, maintained on a 12-hour lightness–darkness cycle, and provided with regular tap water and standard rat chow. A total of 30 young (3-month-old) male Sprague–Dawley rats were used in the study, and they were randomly divided into 4 groups with the following treatments:

- Control group (n = 6): Saline was administered subcutaneously for 10 weeks.
- D-Gal group (n = 8): D-galactose dissolved in saline (150 mg/kg/day) was administered subcutaneously for 10 weeks.
- D-Gal + 4% dimethyl sulfoxide (DMSO) group (n = 8): D-galactose (150 mg/kg/day) and DMSO in phosphate-buffered saline (PBS) (10 μ L/kg/day) were administered subcutaneously for 10 weeks.
- D-Gal + the SIRT2 inhibitor (AGK2) group (n = 8): D-galactose (150 mg/kg/day) and AGK2 prepared in 4% DMSO-PBS (10 μ M/kg/day) were administered subcutaneously for 10 weeks.

AGK2 is a selective SIRT2 inhibitor. It inhibits cell proliferation and cell growth in a dose-dependent manner without inducing cytotoxicity at low doses.²⁹

There was no animal loss during the follow-up period. At the end of the follow-up time, under ketamine/xylazine anesthesia, intracardiac blood samples were collected from the sacrificed rats, and their hearts were removed.

HIGHLIGHTS

- Sirtuin 2 levels were elevated in D-Gal-induced cardiac fibrosis.
- The application of AGK2, a specific sirtuin 2 inhibitor, resulted in decreased levels of sirtuin 2, TGF- β 1, and β -catenin.
- In the future, targeting sirtuin 2 inhibition could be explored as a potential therapeutic strategy for the prevention of fibrosis in many cardiac disorders.

After taking histology samples, the hearts were placed in liquid nitrogen and stored at -80°C until the end of the experiment.

The study protocol was approved by the Local Ethics Committee (Date: June 16, 2023, Decision No.: E-66332047-604.01.02-684514) and was performed in accordance with ethical rules and principles of the "Guiding Principles for the Care and Use of Animals (2011)."

Quantitative Real-Time Polymerase Chain Reaction

First, total RNA isolation (Macherey-Nagel NucleoSpin® RNA Mini Isolation Kit, 50 preps, 740955.50) was performed from all heart tissues. Samples with an optical density of 1.8-2.0 were considered pure, and cDNA was amplified (BIO-RAD, iScript™ cDNA Synthesis Kit, 100 × 20 µL rxn, 1708891) from these samples. Subsequently, amplification was performed in Real-Time PCR using TaqMan primers/probes targeting TGF-β1 and β-catenin genes. The $2^{-\Delta\Delta\text{Ct}}$ method was employed to determine the relative expression levels of the investigated genes. The primer sequences for the target genes are available in Table 1.

Western Blotting

Total protein measurement in tissues homogenized with RIPA Lysis Buffer containing protease and phosphatase inhibitor mixtures was performed with the BCA Protein Assay Kit (Pierce BCA Protein Assay Kit, lot#UD282967, ThermoScientific, IL, USA). Equal amounts of protein (20 µg) from all samples were separated by sodium dodecyl sulfate polyacrylamide gel electrophoresis (SDS-PAGE, 12%) and then transferred to a nitrocellulose membrane (Bio-Rad, Germany). The membrane was incubated with 5% skim milk powder in Tris Buffered Saline-Tween 20 (TBST) at $+4^{\circ}\text{C}$ overnight. Membranes were coated with primary antibodies (Anti-SIRT2, 1:500, sc-28298, Santa Cruz Biotechnology, Dallas, TX, USA; anti-beta-actin, 1:500, sc-47778, Santa Cruz Biotechnology, Dallas, TX, USA), respectively, and incubated with horseradish peroxidase (HRP)-conjugated secondary antibody (Anti-mouse, 1:2000, Cat. #62-6520, Invitrogen, Thermo Fisher Scientific Inc., Cambridge, MA, USA) for 1.5 hours. A chemiluminescence kit (ECL Western Blotting Substrate, Pierce™ ThermoScientific, IL, USA) was used to make the protein bands on the membranes visible. The iBright™ imaging system (# FL 1500, Thermo Fisher

Scientific Inc., MA, USA) was used to visualize and analyze the bands.

Histological Analyzes

All heart samples from the experimental groups were fixed in 10% formaldehyde for 24 hours, then embedded in paraffin, and 4 µm thick sections were taken (Slee, CUT 5062, Germany). Hematoxylin-Eosin (H&E) and Masson's trichrome (Masson) staining were applied to the sections. The prepared preparations were viewed on a ZEISS Axiolab 5 (Germany) computer-assisted light microscope and evaluated in the Zen Blue 3.4 program. Cardiomyocyte diameter and fibrosis percentage were measured using the ImageJ program.

The researchers were unaware of the results of each Western blotting, histological evaluation, and PCR study, but correlations were made after the experiments were completed. The principal author conducted the evaluation.

Statistical Analysis

SPSS 22 software (IBM SPSS Statistics, Chicago, IL, USA) was used to analyze the data. All data were presented as "mean ± SD" on a group basis. The normality of the variables was assessed using visual methods (histogram and probability plots) and analytical methods (Kolmogorov-Smirnov/Shapiro-Wilk tests). All continuous variables across the groups demonstrated a normal distribution; thus, one-way analysis of variance (ANOVA) was employed to assess differences between the groups. Post hoc Tukey's Honestly Significant Difference (HSD) tests were conducted for pairwise comparisons of variables with significant *P*-values in the ANOVA analysis. Pearson's correlation coefficient (*r*) was calculated to determine the correlations between the variables. A level of *P* < .05 was considered statistically significant.

We have not utilized any artificial intelligence (AI)-assisted technologies in the production of the submitted work.

RESULTS

Transforming Growth Factor-Beta 1 and β-catenin mRNA Expression

Transforming growth factor-beta 1 mRNA expression in heart tissue was significantly higher in the D-Gal group

Table 1. Primer Sequences for qPCR

Gene			Base Pair
TGF-β1	Forward (5'-3')	CGCAACAACGCAATCTATGAC	21
	Reverse (5'-3')	TGTTGCTCCACAGTTGACTTG	21
	Probe (5' FAM-3' TAMRA)	CAGTGCCAGAACCCCATTTGCTGTCC	26
β-catenin	Forward (5'-3')	TACGAGAAGCTCCTGTGGAC	20
	Reverse (5'-3')	GCTGCATCGGACAAGTTTCT	20
	Probe (5' FAM-3' TAMRA)	CATCGTGAAGCTGGTGGGATGCAGG	26
β-actin	Forward (5'-3')	TGTCACCAACTGGGACGAT	19
	Reverse (5'-3')	GGGGTGTGTAAGGTCTCAAAC	21
	Probe (5' FAM-3' TAMRA)	CACTTCTACAATGAGCTGCGTGTGG	26

β-catenin, beta-catenin; β-actin, beta-actin; TGF-β1, transforming growth factor-beta 1.

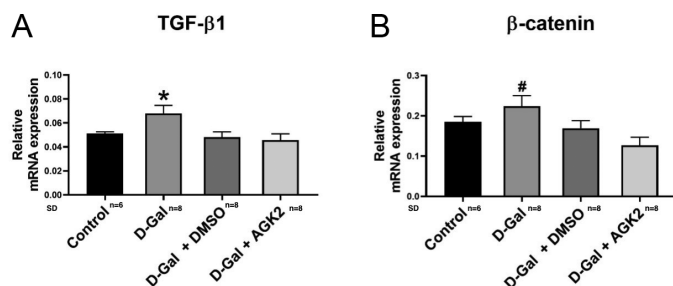


Figure 1. Relative mRNA expression of transforming growth factor-beta 1 (A) (TGF-β1) and (B) β-catenin in heart tissue among groups. *Transforming growth factor-beta 1 mRNA expression was significantly higher in the D-Gal group compared to the control, D-Gal+DMSO, and D-Gal+AGK2 groups ($P=.04$, $P=.01$, $P=.004$, respectively). #β-catenin mRNA expression was higher in the D-Gal group than the D-Gal+AGK2 group ($P=.002$).

compared to all other groups (control, D-Gal+DMSO, D-Gal+AGK2) ($P=.048$, $P=.047$, $P=.021$, respectively) (Figure 1A). β-catenin mRNA expression was higher in the D-Gal group than the D-Gal+AGK2 group ($P=.012$) (Figure 1B) (Table 2).

Sirtuin 2 Protein Expression

Sirtuin 2 protein expression was higher in the D-Gal + DMSO group compared to the control group ($P=.047$). Sirtuin 2 expression was lower in the D-Gal + AGK2 group compared to the D-Gal and D-Gal + DMSO groups ($P=.046$, $P=.033$, respectively) (Figure 2A and B) (Table 2).

Histopathological Findings

The myocardium in the heart sections of the control group and D-Gal+DMSO groups showed a normal histological appearance after H&E staining. In the D-Gal group, irregular cardiomyocyte placement and wide gaps in the interstitial area were observed. It was noted that the cardiomyocytes were in a slightly more regular form in the D-Gal+AGK2 group (Figure 3A).

Cardiomyocyte diameter evaluated by H&E staining in the D-Gal group was significantly larger compared to the control, D-Gal+DMSO, and D-Gal+AGK2 groups ($P < .001$, $P < .001$, $P < .001$, respectively). Additionally, cardiomyocyte diameter was greater in the D-Gal + AGK2 group compared to the control and D-Gal+DMSO groups ($P < .001$, $P < .001$, respectively). No significant difference was found between

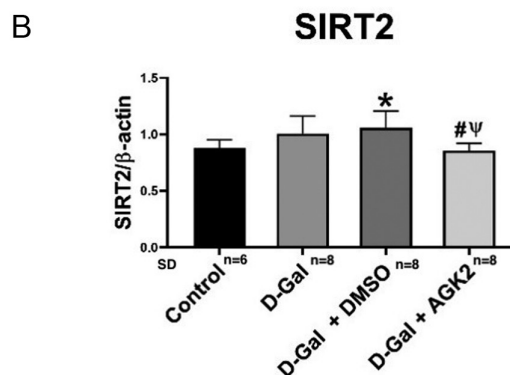
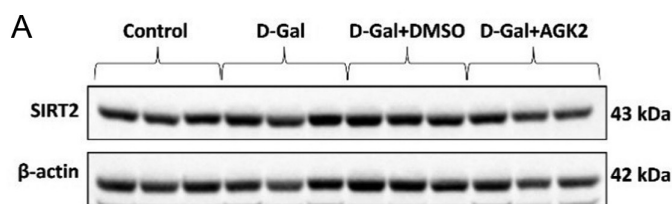


Figure 2. Representative western blots for (A) SIRT2 and β-actin, and (B) relative SIRT2 protein expression in heart tissue among groups. *Sirtuin 2 expression was higher in the D-Gal + DMSO group compared to the control group ($P=.015$). #ψSIRT2 expression was lower in the D-Gal+AGK2 group compared to the D-Gal and D-Gal+DMSO groups ($P=.039$, $P=.007$, respectively).

the control and D-Gal + DMSO groups ($P=.494$) (Figure 3B) (Table 2).

Importantly, our analyses conducted after Masson staining demonstrated a significant increase in the percentage of fibrotic areas in the D-Gal group compared to the control, D-Gal + DMSO, and D-Gal + AGK2 groups ($P < .001$, $P < .001$, $P < .001$, respectively). Notably, the percentage of fibrotic areas in the D-Gal + AGK2 group was higher than in the control and D-Gal + DMSO groups ($P < .001$, $P < .001$, respectively). However, it is worth mentioning that there was no significant difference between the control and D-Gal + DMSO groups ($P=.993$) (Figure 3C) (Table 2).

Additionally, a positive correlation was found between the percentage of fibrotic area and cardiomyocyte diameter ($r = 0.868$, $P < .001$). A positive correlation was also found

Table 2. Mean, SD, and ANOVA Results (F and P Values) for Study Groups

	Control (n=6)	D-Gal (n=8)	D-Gal + DMSO (n=8)	D-Gal + AGK2 (n=8)	ANOVA
TGF-β1 (mRNA)	0.05 ± 0.003	0.07 ± 0.016	0.05 ± 0.011	0.05 ± 0.014	$F(3,26) = 3.986$; $P=.022$
β-catenin (mRNA)	0.19 ± 0.03	0.22 ± 0.06	0.17 ± 0.05	0.13 ± 0.05	$F(3,26) = 4.095$; $P=.020$
SIRT2/β-actin	0.88 ± 0.07	1.01 ± 0.16	1.06 ± 0.15	0.86 ± 0.06	$F(3,26) = 4.186$; $P=.019$
Cardiomyocyte diameter (μm)	15.81 ± 1.01	23.97 ± 0.40	16.88 ± 1.43	20.26 ± 2.04	$F(3,26) = 52.565$; $P < .001$
Fibrotic area (%)	0.83 ± 0.15	9.25 ± 1.61	1.02 ± 0.37	5.43 ± 1.97	$F(3,26) = 67.942$; $P < .001$

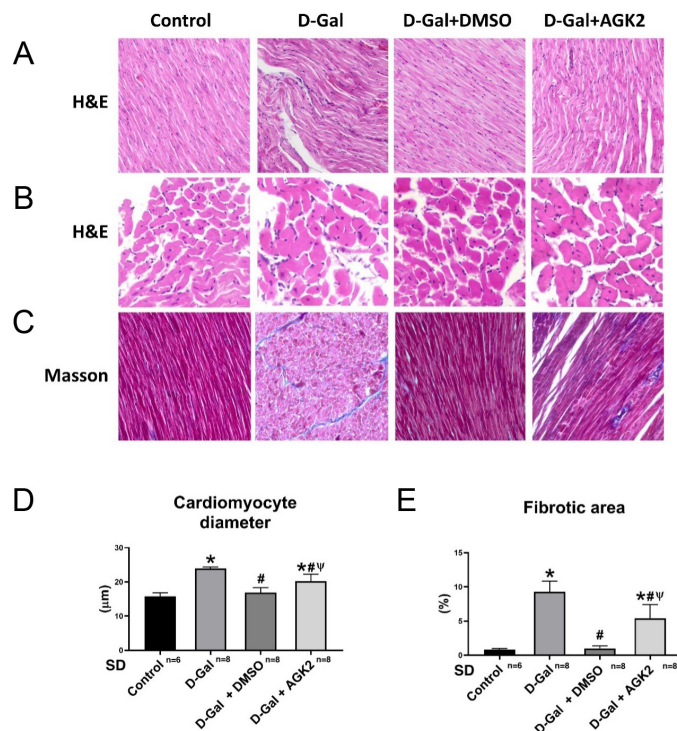


Figure 3. Representative staining micrographs of (A, B) Hematoxylin–Eosin (H&E, $\times 200$) and (C) Masson's Trichrome (Masson, $\times 200$). The evaluation of (D) cardiomyocyte diameter and (E) fibrotic area. Cardiomyocytes were in a slightly more regular form in the D-Gal + AGK2 group (A). The cardiomyocyte diameter (B, D) and the percentage of fibrotic area (C, E) were *higher in the D-Gal and D-Gal+AGK2 groups compared to the control group ($P < .001$, $P < .001$, respectively); #lower in the D-Gal + DMSO and D-Gal + AGK2 groups compared to the D-Gal group ($P < .001$, $P < .001$, respectively); and vhigher in the D-Gal+AGK2 group compared to the D-Gal+DMSO group ($P < .001$). No significant differences were observed in cardiomyocyte diameter and percentage of fibrotic area between the control and D-Gal+DMSO groups ($P = .165$, $P = .795$, respectively).

between TGF- $\beta 1$ mRNA expression and cardiomyocyte diameter and fibrotic area percentage ($r = 0.47$, $P = .018$; $r = 0.442$, $P = .027$, respectively).

DISCUSSION

D-Galactose, a monosaccharide, contributes to the formation of ROS, induces organ aging, and shortens lifespan through the accumulation of galactitol in the body.¹² Numerous studies have demonstrated that D-Gal-induced cardiac aging models exhibit cardiac hypertrophy, increased inflammatory cell infiltration in the heart, and fatty tissue hyperplasia.^{3,12}

Administering D-Gal at various doses and durations (100–400 mg/kg for 6–8 weeks) led to a reduction in the ejection fraction and fractional shortening of the rat heart.^{12,30–32} Structurally, there was an increase in left ventricular end-diastolic posterior wall thickness and left ventricular

end-systolic volume.^{12,31} These findings indicate impaired diastolic function and the development of an age-related dilated cardiomyopathy model.^{5,6}

To maintain the morphology and function of the aging heart, fibroblasts differentiate into myofibroblasts, leading to the accumulation of extracellular matrix proteins in the interstitium.^{32,33} This process contributes to progressive fibrosis, tissue stiffening, and heart failure, which can disrupt the electrical conduction system of the heart. Increased myocardial TGF- $\beta 1$ expression has been observed during cardiac hypertrophy and fibrosis in humans and experimental models.^{12,17} Collagen deposition and elevated TGF- β levels in the heart contribute to fibrosis.²⁹

It has previously been shown that D-Gal administration increases TGF- $\beta 1$ mRNA, β -catenin mRNA expression, immunoreactivity, and fibronectin immunoreactivity in kidney and liver tissues, while reducing klotho levels in the kidney.^{20,21}

Chronic Wnt signaling activation has been shown to induce the transformation of fibroblasts into activated fibroblasts or myofibroblasts, contributing to cardiac fibrosis in aged hearts.^{34,35} D-Galactose administration triggers fibrogenesis by promoting the nuclear translocation of β -catenin, a downstream effector of Wnt signaling.³⁶ Increased β -catenin mRNA and protein expression has been observed in the intestinal cells³⁷ and kidneys³⁸ of D-Gal-treated mice.

Our study revealed that TGF- $\beta 1$ and β -catenin expression in heart tissue significantly increased following D-Gal treatment compared to other groups (Figure 1). This increase was consistent with the histological analysis performed after Masson staining (Figure 3). Dimethyl sulfoxide was primarily employed as a solvent for AGK2 in this study; however, its well-documented anti-inflammatory and anti-fibrotic effects are also noteworthy.^{39,40} Accordingly, we observed a reduction in TGF- $\beta 1$ expression in the D-Gal+DMSO group compared to the D-Gal group. No significant difference in TGF- $\beta 1$ expression was detected between the D-Gal + DMSO and D-Gal + AGK2 groups. Interestingly, while β -catenin expression remained comparable between the D-Gal and D-Gal + DMSO groups, it was markedly lower in the D-Gal + AGK2 group, demonstrating the independent anti-fibrotic effect of SIRT2 inhibition.

The percentage of fibrotic areas was significantly higher in the D-Gal group compared to the control, D-Gal+DMSO, and D-Gal+AGK-2 groups. In the D-Gal group, irregular cardiomyocyte arrangement and interstitial area widening were observed. Cardiomyocytes appeared more regular in the D-Gal + AGK2 group. These findings are consistent with previous studies that reported vacuolization, intracellular edema, and cardiomyocyte expansion as indicators of cardiac damage in D-Gal models.^{3,7,12,31,41,42} Cheng et al³¹ also noted collagen accumulation in the myocardium's perivascular and interstitial areas. Additionally, aging increases cardiomyocyte diameter but decreases their number, accompanied by significant collagen deposition.⁴³ Histological analysis also showed SIRT2 deletion and smaller cardiomyocytes in hearts exposed to high pressure.²¹ Interestingly, the percentage of

fibrotic area observed in the D-Gal + DMSO group was similar to that of the control group. We believe that this phenomenon is likely attributable to the anti-fibrotic effects of DMSO.

Sirtuin 2 is expressed in all mammalian cells and has been linked to anti-aging and antioxidant properties. However, it can also exacerbate ischemia-reperfusion injury in the heart.⁴⁴ The effects of SIRT2 are bidirectional; low levels are protective against oxidative stress, while high levels may be detrimental.⁴⁴

Sirtuin 2's role in inflammation and fibrosis varies across different tissues such as the liver, heart, and kidney.^{22,45,46} For instance, SIRT2 provides cardioprotection in age-related or angiotensin II-induced cardiac hypertrophy, with SIRT2 knockout exacerbating these conditions. Conversely, in the liver and kidney, SIRT2 promotes fibrogenesis, and its inhibition suppresses fibrosis and inactivates liver stellate cells and kidney fibroblasts.^{35,45} D-galactose administration has been shown to increase SIRT2 expression in kidney,²¹ liver²⁰ and brain tissues.⁴⁷

In heart failure, increased levels of SIRT2, among other sirtuin family members, were observed in heart tissue, with significant increases noted in patients with end-stage heart failure and dilated cardiomyopathy. Elevated SIRT2 levels were also found in ischemic cardiomyopathy patients' heart tissue.⁴³

Tang and colleagues showed that SIRT2 levels decrease in age-related or stress-induced cardiac hypertrophy, and SIRT2 knockout exacerbates this pathology, while SIRT2 overexpression has ameliorative effects.²² Likewise, Chen et al⁴⁸ have shown that overexpression of SIRT2 down-regulates the expression of several collagens and MMPs, reducing the fibrotic area in the heart tissues of mice with radiation exposure.

On the other hand, SIRT2 is induced by anoxia-reoxygenation in heart-derived H9c2 cells, where its overexpression increases cell death via deacetylase activity, and SIRT2 deletion enhances tolerance to anoxia-reoxygenation and oxidative stress.²⁵ Research on calcific aortic valve stenosis pathogenesis has also identified matrix metalloproteinase-1 and SIRT2 as potential therapeutic targets.⁴³ Similarly, Gong et al⁴⁹ demonstrated that SIRT2 expression is upregulated in human fibroblasts treated with TGF- β 1 and that the administration of AGK2 suppressed the expression of fibrogenic genes, like fibronectin. Likewise, our study revealed that D-Gal and D-Gal + DMSO treatments elevated SIRT2 levels, while the lowest SIRT2 expression was observed in the D-Gal + AGK2 group, mirroring the expression patterns of TGF- β 1 and β -catenin. These findings suggest that SIRT2 plays a central role in cardiac fibrotic signaling pathways, and its inhibition down-regulates TGF- β and Wnt/ β -catenin pathways, consequently reducing the fibrotic area in the hearts of the D-gal-treated rats.

Although DMSO is classified as a safe solvent by the Food and Drug Administration, it has been shown to cause tissue-specific epigenomic changes, particularly in methylation and microRNA (miRNA) studies. Verheijen et al⁵⁰ found that

DMSO affects miRNAs in a maturing heart model, causing significant epigenetic changes. While our previous studies with DMSO did not show epigenetic effects in brain and heart tissues, Verheijen et al observed effects specifically in heart tissue, but not in the liver. Therefore, the increase in SIRT2 levels in heart tissue due to DMSO could be attributed to a tissue-specific response.

Study Limitations

Owing to the small body size of the rats, we were unable to isolate the left ventricle for assessing the fibrosis of cardiac tissue and therefore, utilized the whole heart for tissue analysis. This is one of the main limitations of our study. Moreover, the reliability of our findings is somewhat limited by the fact that the molecular and histological assessments were not performed by multiple observers.

CONCLUSION

Fibrosis is a fundamental characteristic of a variety of cardiac diseases and aging. The TGF- β and Wnt/ β -catenin signaling pathways are central to the development of interstitial cardiac fibrosis. SIRT2, 1 of the 7 class III histone deacetylases, appears to be essential for the activation of fibroblasts, and its inhibition may reduce TGF- β -induced fibroblast activation and extracellular matrix production. Our findings suggest that targeting the pharmacological inhibition of SIRT2 may represent a promising therapeutic strategy for the treatment of cardiac fibrosis across multiple cardiac disease states.

Ethics Committee Approval: Ethical approval was obtained from the Gazi University Local Ethics Committee for Animal Experiments (G.U.ET-23.062), and the procurement and care of the rats were managed at the Gazi University Experimental Animals Research and Application Center (Ethics Committee Decision Date: June 16, 2023, Decision Number: E-66332047-604.01.02-684514).

Peer-review: Externally peer-reviewed.

Author Contributions: Concept – A.A.K.; Design – A.A.K.; Data collection or processing – G.F.S., A.B.O., H.K.; Analysis or Interpretation – G.F.S., K.G.A.; Literature search – G.F.S., A.B.O.; Writing – M.A.; Approval – K.G.A.

Declaration of Interests: The authors have no conflicts of interest to declare.

Funding: The authors declare that this study received no financial support.

REFERENCES

1. Sacco RL, Roth GA, Reddy KS, et al. The heart of 25 by 25: achieving the goal of reducing global and regional premature deaths from cardiovascular diseases and stroke: a modeling study from the American Heart Association and World Heart Federation. *Circulation*. 2016;133(23):e674-e690. [CrossRef]
2. Murtha LA, Morten M, Schuliga MJ, et al. The role of pathological aging in cardiac and pulmonary fibrosis. *Aging Dis*. 2019;10(2):419-428. [CrossRef]
3. Cebe T, Yanar K, Atukeren P, et al. A comprehensive study of myocardial redox homeostasis in naturally and mimetically aged rats. *Age (Dordr)*. 2014;36(6):9728. [CrossRef]

4. Aydin S, Yanar K, Atukeren P, et al. Comparison of oxidative stress biomarkers in renal tissues of D-galactose induced, naturally aged and young rats. *Biogerontology*. 2012;13(3):251-260. [\[CrossRef\]](#)
5. Hong YX, Wu WY, Song F, Wu C, Li GR, Wang Y. Cardiac senescence is alleviated by the natural flavone acacetin via enhancing mitophagy. *Aging (Albany NY)*. 2021;13(12):16381-16403. [\[CrossRef\]](#)
6. Li HM, Liu X, Meng ZY, et al. Kanglexin delays heart aging by promoting mitophagy. *Acta Pharmacol Sin*. 2022;43(3):613-623. [\[CrossRef\]](#)
7. Bo-Htay C, Shwe T, Higgins L, et al. Aging induced by D-galactose aggravates cardiac dysfunction via exacerbating mitochondrial dysfunction in obese insulin-resistant rats. *GeroScience*. 2020;42(1):233-249. [\[CrossRef\]](#)
8. Biernacka A, Frangogiannis NG. Aging and cardiac fibrosis. *Aging Dis*. 2011;2(2):158-173.
9. Murtha LA, Schuliga MJ, Mabotuwana NS, et al. The processes and mechanisms of cardiac and pulmonary fibrosis. *Front Physiol*. 2017;8(8):777. [\[CrossRef\]](#)
10. Kuwahara F, Kai H, Tokuda K, et al. Transforming growth factor-beta function blocking prevents myocardial fibrosis and diastolic dysfunction in pressure-overloaded rats. *Circulation*. 2002;106(1):130-135. [\[CrossRef\]](#)
11. Villarreal FJ, Dillmann WH. Cardiac hypertrophy-induced changes in mRNA levels for TGF-beta 1, fibronectin, and collagen. *Am J Physiol*. 1992;262(6 Pt 2):H1861-H1866. [\[CrossRef\]](#)
12. Chang YM, Chang HH, Lin HJ, et al. Inhibition of cardiac hypertrophy effects in D-galactose-induced senescent hearts by Alpinate Oxyphyllae fructus treatment. *Evid Based Complement Alternat Med*. 2017;2017:2624384. [\[CrossRef\]](#)
13. Khalil H, Kanisicak O, Prasad V, et al. Fibroblast-specific TGF- β -Smad2/3 signaling underlies cardiac fibrosis. *J Clin Invest*. 2017;127(10):3770-3783. [\[CrossRef\]](#)
14. Liu H, Fergusson MM, Castilho RM, et al. Augmented Wnt signaling in a mammalian model of accelerated aging. *Science*. 2007;317(5839):803-806. [\[CrossRef\]](#)
15. Naito AT, Shiojima I, Komuro I. Wnt signaling and aging-related heart disorders. *Circ Res*. 2010;107(11):1295-1303. [\[CrossRef\]](#)
16. Dawson K, Aflaki M, Nattel S. Role of the Wnt-Frizzled system in cardiac pathophysiology: a rapidly developing, poorly understood area with enormous potential. *J Physiol*. 2013;591(6):1409-1432. [\[CrossRef\]](#)
17. Działo E, Tkacz K, Błyszczuk P. Crosstalk between the TGF- β and WNT signalling pathways during cardiac fibrogenesis. *Acta Biochim Pol*. 2018;65(3):341-349. [\[CrossRef\]](#)
18. Działo E, Czepiel M, Tkacz K, Siedlar M, Kania G, Błyszczuk P. WNT/ β -catenin signaling promotes TGF- β -mediated activation of human cardiac fibroblasts by enhancing IL-11 production. *Int J Mol Sci*. 2021;22(18):10072. [\[CrossRef\]](#)
19. Garg G, Singh S, Singh AK, Rizvi SI. Antiaging effect of metformin on brain in naturally aged and accelerated senescence model of rat. *Rejuvenation Res*. 2017;20(3):173-182. [\[CrossRef\]](#)
20. Bahar AN, Keskin Aktan A, Sonugür FG, Akarca Dizakar SÖ, Akbulut KG. "Effect of SIRT2 Inhibition on Developing Fibrosis in D-Galactose-Induced Aging Model", 47th Turkish Physiology Congress, Antalya, Türkiye: 1-4 November 2022; 237(727):22.
21. Keskin-Aktan A, Bahar AN, Sonugür FG, Akarca-Dizakar SO, Akbulut KG. Protective effect of pharmacological SIRT2 inhibition on renal dysfunction, fibrosis, TGF- β 1/ β -catenin, and klotho signaling in D-galactose-induced aging model. *J Biol Regul Homeost Agents*. 2023;37(11):6061-6072.
22. Tang X, Chen XF, Wang NY, et al. SIRT2 acts as a cardioprotective deacetylase in pathological cardiac hypertrophy. *Circulation*. 2017;136(21):2051-2067. [\[CrossRef\]](#)
23. Sarikhani M, Maity S, Mishra S, et al. SIRT2 deacetylase represses NFAT transcription factor to maintain cardiac homeostasis. *J Biol Chem*. 2018;293(14):5281-5294. [\[CrossRef\]](#)
24. Taneja A, Ravi V, Hong JY, Lin H, Sundaresan NR. Emerging roles of sirtuin 2 in cardiovascular diseases. *FASEB J*. 2021;35(10):e21841. [\[CrossRef\]](#)
25. Lynn EG, McLeod CJ, Gordon JP, Bao J, Sack MN. SIRT2 is a negative regulator of anoxia-reoxygenation tolerance via regulation of 14-3-3 zeta and BAD in H9c2 cells. *FEBS Lett*. 2008;582(19):2857-2862. [\[CrossRef\]](#)
26. Sundaresan NR, Bindu S, Pillai VB, et al. SIRT3 blocks aging-associated tissue fibrosis in mice by deacetylating and activating glycogen synthase kinase β . *Mol Cell Biol*. 2015;36(5):678-692. [\[CrossRef\]](#)
27. Wołowicz A, Wołowicz Ł, Grzešek G, et al. The role of selected epigenetic pathways in cardiovascular diseases as a potential therapeutic target. *Int J Mol Sci*. 2023;24(18):13723. [\[CrossRef\]](#)
28. Zhu L, Li C, Liu Q, Xu W, Zhou X. Molecular biomarkers in cardiac hypertrophy. *J Cell Mol Med*. 2019;23(3):1671-1677. [\[CrossRef\]](#)
29. Tatum PR, Sawada H, Ota Y, et al. Identification of novel SIRT2-selective inhibitors using a click chemistry approach. *Bioorg Med Chem Lett*. 2014;24(8):1871-1874. [\[CrossRef\]](#)
30. Bei Y, Wu X, Cretoiu D, et al. miR-21 suppression prevents cardiac alterations induced by d-galactose and doxorubicin. *J Mol Cell Cardiol*. 2018;115:130-141. [\[CrossRef\]](#)
31. Cheng J, Ren C, Cheng R, et al. Mangiferin ameliorates cardiac fibrosis in D-galactose-induced aging rats by inhibiting TGF- β /p38/MK2 signaling pathway. *Korean J Physiol Pharmacol*. 2021;25(2):131-137. [\[CrossRef\]](#) Erratum in: *Korean J Physiol Pharmacol*. 2021;25(3):259. (<https://doi.org/10.4196/kjpp.2021.25.3.259>)
32. Alejandro SP. ER stress in cardiac aging, a current view on the D-galactose model. *Exp Gerontol*. 2022;169:111953. [\[CrossRef\]](#)
33. Horn MA, Trafford AW. Aging and the cardiac collagen matrix: novel mediators of fibrotic remodelling. *J Mol Cell Cardiol*. 2016;93:175-185. [\[CrossRef\]](#)
34. Königshoff M, Kramer M, Balsara N, et al. WNT1-inducible signaling protein-1 mediates pulmonary fibrosis in mice and is upregulated in humans with idiopathic pulmonary fibrosis. *J Clin Invest*. 2009;119(4):772-787. [\[CrossRef\]](#)
35. He W, Dai C, Li Y, Zeng G, Monga SP, Liu Y. Wnt/ β -catenin signaling promotes renal interstitial fibrosis. *J Am Soc Nephrol*. 2009;20(4):765-776. [\[CrossRef\]](#)
36. Li J, Cai D, Yao X, et al. Protective effect of ginsenoside Rg1 on hematopoietic stem/progenitor cells through attenuating oxidative stress and the Wnt/ β -catenin signaling pathway in a mouse model of d-galactose-induced aging. *Int J Mol Sci*. 2016;17(6):849. [\[CrossRef\]](#)
37. Guo LL, Yan RY, Du Z, Li HB, Li GL, Wu SH. Ginseng promotes the function of intestinal stem cells through the Wnt/ β -catenin signaling pathway in D-galactose-induced aging mice. *Exp Gerontol*. 2024;185:112351. [\[CrossRef\]](#)
38. Miao J, Liu J, Niu J, et al. Wnt/ β -catenin/RAS signaling mediates age-related renal fibrosis and is associated with mitochondrial dysfunction. *Aging Cell*. 2019;18(5):e13004. [\[CrossRef\]](#) Erratum in: *Aging Cell*. 2023;22(5):e13816. (<https://doi.org/10.1111/ace13816>)
39. Nakamuta M, Ohta S, Tada S, et al. Dimethyl sulfoxide inhibits dimethylnitrosamine-induced hepatic fibrosis in rats. *Int J Mol Med*. 2001;8(5):553-560. [\[CrossRef\]](#)
40. Leon AS, White FC, Bloor CM, Saviano MA. Reduced myocardial fibrosis after dimethylsulfoxide (DMSO) treatment of

- isoproterenol-induced myocardial necrosis in rats. *Am J Med Sci*. 1971;261(1):41-45. [\[CrossRef\]](#)
41. Ji M, Su X, Liu J, et al. Comparison of naturally aging and D-galactose induced aging model in beagle dogs. *Exp Ther Med*. 2017;14(6):5881-5888. [\[CrossRef\]](#)
 42. Shahidi S, Ramezani-Aliakbari K, Komaki A, et al. Effect of vitamin D on cardiac hypertrophy in D-galactose-induced aging model through cardiac mitophagy. *Mol Biol Rep*. 2023;50(12):10147-10155. [\[CrossRef\]](#)
 43. Bernhard D, Laufer G. The aging cardiomyocyte: a mini-review. *Gerontology*. 2008;54(1):24-31. [\[CrossRef\]](#)
 44. Yang X, Chang HC, Tatekoshi Y, et al. SIRT2 inhibition protects against cardiac hypertrophy and ischemic injury. *eLife*. 2023;12:e85571. [\[CrossRef\]](#)
 45. Ponnusamy M, Zhou X, Yan Y, et al. Blocking sirtuin 1 and 2 inhibits renal interstitial fibroblast activation and attenuates renal interstitial fibrosis in obstructive nephropathy. *J Pharmacol Exp Ther*. 2014;350(2):243-256. [\[CrossRef\]](#)
 46. Arteaga M, Shang N, Ding X, et al. Inhibition of SIRT2 suppresses hepatic fibrosis. *Am J Physiol Gastrointest Liver Physiol*. 2016;310(11):G1155-G1168. [\[CrossRef\]](#)
 47. Singh S, Singh AK, Garg G, Rizvi SI. Fisetin as a caloric restriction mimetic protects rat brain against aging induced oxidative stress, apoptosis and neurodegeneration. *Life Sci*. 2018;193:171-179. [\[CrossRef\]](#)
 48. Chen L, Cai X, Shao L, Wang Y, Hong L, Zhan Y. Sirtuin 2 exerts regulatory functions on radiation-induced myocardial fibrosis in mice by mediating H3K27 acetylation of galectin-3 promoter. *Acta Cardiol Sin*. 2024;40(2):214-224. [\[CrossRef\]](#)
 49. Gong H, Zheng C, Lyu X, Dong L, Tan S, Zhang X. Inhibition of Sirt2 alleviates fibroblasts activation and pulmonary fibrosis via Smad2/3 pathway. *Front Pharmacol*. 2021;12:756131. [\[CrossRef\]](#)
 50. Verheijen M, Lienhard M, Schrooders Y, et al. DMSO induces drastic changes in human cellular processes and epigenetic landscape in vitro. *Sci Rep*. 2019;9(1):4641. [\[CrossRef\]](#)